RSC Advances

Volume 1 | Number 1 | Jan 2013 | Pages 1–100

RSC Advances

www.rsc.org/advances

ROYAL SOCIETY OF CHEMISTRY

ROYAL SOCIETY OF CHEMISTRY

www.rsc.org/advances

5-HT$_6$R ligands database

Bioisostere query

5 commercial compounds databases

Bioisosteric substituton

Hit compound

Lead

5-HT$_6$R
$K_i = 6$ nM

Crystallographic and molecular modelling studies

RSC Advances

ARTICLE TYPE

Rational design of 5-HT$_6$R ligands using a bioisosteric strategy: Synthesis, biological evaluation and molecular modelling

Jakub Staroń,[a] **Dawid Warszycki**[a]**, Justyna Kalinowska-Tłuścik,** [b] **Grzegorz Satała**[a] **and Andrzej J. Bojarski**[a]*****

[a]*Department of Medicinal Chemistry, Institute of Pharmacology Polish Academy of Sciences*
12 Smętna Street, 31-343 Kraków, Poland
[b]*Department of Crystal Chemistry and Crystal Physic, Jagiellonian University Faculty of Chemistry*
3 R. Ingardena Street, 30-060 Kraków, Poland
*Corresponding author: Institute of Pharmacology PAS, Kraków. Tel. +48 12 6623365, email: bojarski@if-pan.krakow.pl

A bioisosteric strategy was successfully implemented with a screening protocol for new, potent 5-HT$_6$R ligands. Initially, (2-[5-(4-methylpiperazin-1-yl)-2-nitrophenyl]-1,2,3,4-tetrahydroisoquinoline (**9**) was found in commercial databases using a bioisosteric query (screening 5-HT$_6$R K_i = 128 nM). Then, the hit compound was bioisosterically modified (ring alteration) leading to a novel, high affinity (K_i = 6 nM) 5-HT$_6$R ligand (**10**). Extensive docking studies followed by structural interaction fingerprint analysis supported by single-crystal X-ray structures of the investigated ligands suggest different binding modes with 5-HT$_6$R models for compounds with varying activity. An alternative anchoring point for protonated amine (D7.36) that has not been previously reported was identified.

Keywords: virtual screening, bioisosteric substitution, serotonin receptor, 5-HT$_6$ receptor, 5-HT$_6$R ligands

Introduction

Isosteric or, in the case of biologically active compounds, bioisosteric substitution is one of the most commonly used methods for developing new compounds with required characteristics, e.g., drugs with improved pharmacodynamics and/or pharmacokinetic properties.[1] The first known bioisosteric replacement that revolutionized drug development and medicine was the discovery of Prontosil.[2] Prontosil was the first antibiotic of the sulfonamide family. Its active metabolite, sulfanilamide, is an actual bioisostere of p-aminobenzoic acid, an intermediate in the bacterial synthesis of folate. Since then, this strategy, usually in the context of structure-activity relationship studies, has been widely used in the search for novel active compounds to different biological targets, among others for the modification of serotonin receptor ligands.

One of the first studies concerning bioisosterism in serotonin receptor ligands was published in 1987 and utilized indazoles as indole substitutes in 5-HT$_3$R antagonists.[3] Another report from 1992 described the bioisosteric replacement of indole with benzofuran in a series of 5-HT$_2$R agonists.[4] Twelve years later, a 5-HT$_{1f}$R agonist with an indole–furopyridine ring substitution was reported.[5] The most recent paper, published in 2010, reported the replacement of a benzene ring in haloperidol with [2,2]-paracyclophane.[6] In spite of the large number of reports of bioisosterism, none discuss explicitly the application of nonclassical bioisosteric strategy to 5-HT$_6$ receptor ligands.[7]

The 5-HT$_6$ receptor, a member of the GPCR superfamily, shows significant therapeutic potential and is a promising target for novel psychotropic drugs.[8] This receptor is responsible primarily for motor control, memory and learning, and its antagonists have several applications, e.g., improving cognitive function and memory in cognitive impairments.[9–11] These antagonists are also potential antiobesity drugs.[12,13] The 5-HT$_6$R and some other members of serotonergic receptor family have been investigated in our laboratories for a long time, and this research has included the synthesis of novel ligands, in vitro testing, homology modeling, pharmacophore filtering and multistep virtual screening.[14–18]

In this study, we present an implementation of bioisosteric query to the virtual screening (VS) of potential 5-HT$_6$R ligands in a 5.4 million database of commercial compounds and subsequent bioisosteric modification of the VS hit. All alterations of the hit structure were ring modifications which resulted in the discovery of a new, potent 5-HT$_6$ receptor ligand. To explain differences in 5-HT$_6$R ligands affinity, the single crystal X-ray structure analysis and docking studies were performed.

Initial screening – selection of a hit compound

The hit compound was found from a multistep ligand-based virtual screening cascade performed on compound collections from five vendors with a query based on bioisosteres of 5-HT$_6$R ligands (Figure 1.). The ChEMBL database version 13, extended by data from ca. 30 patents, was used as a source of compounds with known 5-HT$_6$ affinity.[19] For each of the 4298 compounds

from the final set, all possible bioisosteres were generated in Pipeline Pilot.[20] After removal of duplicates, a collection of 137 951 unique compounds was obtained. Next, from the database of 5.4 million commercially available structures (Chembridge, Chemdiv, UORSY, Vitas M and Enamine), those

with Tanimoto similarity coefficients (Tc) higher than or equal to 0.9 to any previously generated bioisostere were fetched, and the resulting set of 1718 analogues was subjected to further filtering steps.
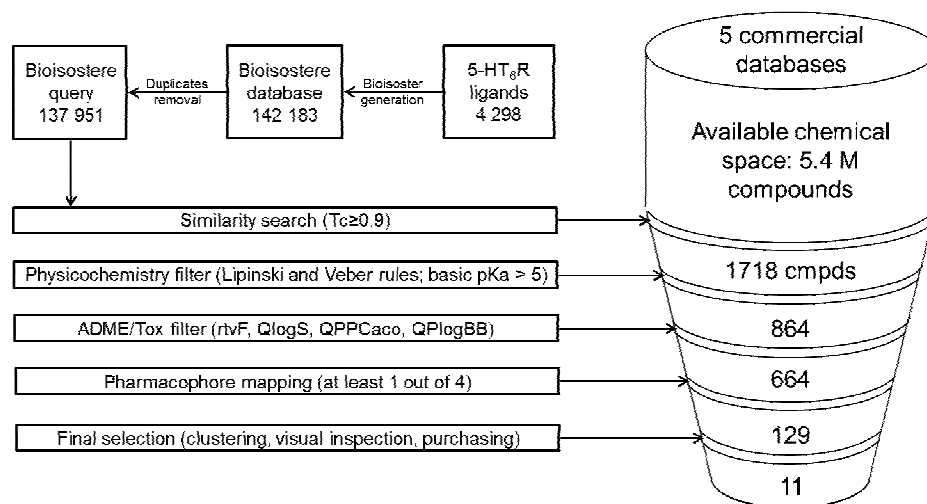

Figure 1 Workflow for the virtual screening protocol with bioisostere query for the identification of a hit compound.

The applied protocol followed the hierarchical scheme reported previously and consisted of four filters: physicochemical, ADME, 3D pharmacophore and visual inspection.[21] First, the Lipinski rules of 5, the Veber rules and the criteria of the strongest basic pKa > 5 were applied (Calculator Plugins, JChem).[22] After generation of 3D structures (Ligprep), the ADME descriptors (QikProp) were calculated, and only compounds fulfilling all ADME requirements (see experimental) were considered.[23,24] In the next phase, a linear combination of four different pharmacophore models, developed using four of the most populated chemical scaffolds of 5-HT$_6$R antagonists (indoles, indole-like, monocyclic arylpiperazines and polycyclic arylpiperazines), were applied.[17] Finally, 129 compounds, each matching at least one of the pharmacophore models, were evaluated by team members to select structures with the most diverse chemotypes for biological investigation. As a result, a set of 11 compounds (Supplementary data) was acquired from Vitas M, Chembridge and Enamine and tested for 5-HT$_6$ receptor activity at two concentrations (see experimental). Of the tested compounds, (2-[5-(4-methylpiperazin-1-yl)-2-nitrophenyl]-1,2,3,4-tetrahydroisoquinoline), STK148877 (**9**), was the most potent (screening 5-HT$_6$R K_i = 128 nM) and was selected as a hit compound for further modification.

Chemistry

The parent of the hit compound, N-benzyl-5-(4-methylpiperazin-1-yl)-2-nitroaniline (**4**), was previously reported by Tasler et al..[25] A modified route of its resynthesis, where instead of coupling of 2-bromo-4-chloronitrobenzene with Boc-protected benzylamine, a coupling of 5-chloro-2-nitroaniline with benzylbromide with subsequent Boc protection was employed. (scheme 1).[26]
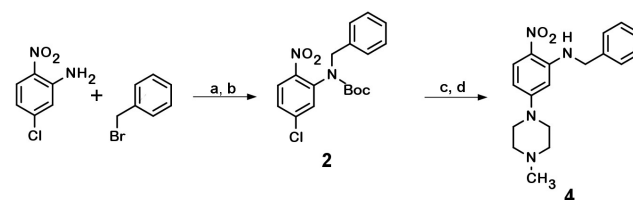
Scheme 1 Synthesis of N-benzyl-5-(4-methylpiperazin-1-yl)-2-nitroaniline (**4**). Reagents and conditions: (a) H$_2$O, reflux, 1,5 h; (b) KHMDS, Boc$_2$O, THF, 0 °C; (c) Pd(OAc)$_2$, JohnPhos, K$_3$PO$_4$•H$_2$O, N-Me-piperazine, DME, 100 °C, 20 h; (d) MeOH, conc. HCl, reflux, 3 h.

Syntheses of the hit compound **9** and its two isosteres (2-[5-(4-methylpiperazin-1-yl)-2-nitrophenyl]-2,3-dihydro-1H-isoindole **8** and 2-[5-(4-methylpiperazin-1-yl)-2-nitrophenyl]-2,3,4,5-tetrahydro-1H-2-benzazepine **10** were performed according to the synthetic route shown in scheme 2. The general procedure utilized coupling of 4-chloro-2-fluoronitrobenzene with amines at the 2-position and subsequent addition of N-Me-piperazine through the Buchwald-Hartwig reaction.
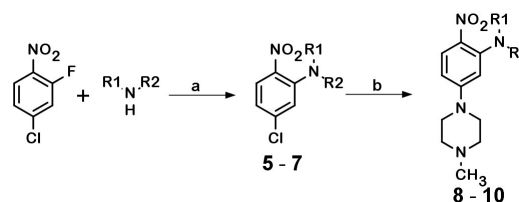
Scheme 2 Synthesis of 4-methylpiperazin-1-yl-2-nitroanilines (**8**, **9**, **10**). Reagents and conditions: (a) DMSO, K$_2$CO$_3$, 120 °C, 2 h; (b) Pd(OAc)$_2$, JohnPhos, K$_3$PO$_4$•H$_2$O, N-Me-piperazine, DME, 100 °C, 20 h.

Pharmacology

In vitro evaluation

Radioligand binding assays were employed to determine the affinity and selectivity profiles of the synthesized compounds for human serotonin 5-HT$_{1A}$R, 5-HT$_6$R, 5-HT$_{7b}$R and D$_{2L}$R, which were stably expressed in HEK293 cells. This was accomplished by displacement of [^{3}H]-8-OH-DPAT (187 Ci/mmol) for 5-HT$_{1A}$R; [^{3}H]-LSD (85.2 Ci/mmol) for 5-HT$_6$R; [^{3}H]-5-CT (39.2 Ci/mmol) for 5-HT$_{7b}$R and [^{3}H]-Raclopride (74.4 Ci/mmol) for D$_{2L}$R. Each compound was tested in triplicate at 7 to 8 different concentrations (10^{-11}–10^{-4} M). The inhibition constants (K_i) were calculated from the Cheng-Prusoff equation.[27] The results are expressed as the mean of at least two separate experiments (Table 1).

Table 1 Affinities of the synthesized compounds.

| R | Cmpd | K_i [nM] | | | | Function at 5-HT$_6$[e] | K_B[e] [nM] |
		5-HT$_{1A}$[a]	5-HT$_6$[b]	5-HT$_7$[c]	D$_2$[d]		
	4	1278	22	2783	557	antagonist	79
	8	2292	245	5117	1396	antagonist	1000
	9[f]	3740	62	4148	227	antagonist	340
	10	1015	6	5181	358	antagonist	29

[a] buspirone as a reference K_i = 20 nM, [b] olanzapine as a reference K_i = 7 nM, [c]clozapine as a reference K_i = 18 nM, [d]olanzapine as a reference K_i = 7 nM, [e]methiotepine as a reference K_B = 3.1 nM, [f]resynthesized STK148877.

The most potent and selective 5-HT$_6$R ligand, 2-[5-(4-methylpiperazin-1-yl)-2-nitrophenyl]-2,3,4,5-tetrahydro-1H-2-benzazepine **10**, was further investigated for other activities by CEREP (Table 2). It is noteworthy that compound **10** was found to be 60-fold selective, versus only 25-fold selectivity for compound **4**, against D$_2$R. Antagonist effect at 5-HT$_6$R was determined by CEREP (Table 1). The parent compound **4**, as well as compounds **8**–**10**, exhibit antagonistic properties of different potency, proportional to 5-HT$_6$ affinity values. Tasler et al. reported the function of analogue of parent compound **4** with unmethylated piperazine to be full agonist.[25] The function of methylated parent compound **4** was not reported but it was shown that similar compound with 2-furane moiety instead of phenyl ring possessed partial agonistic properties.

Table 2 % Inhibition of Specific Binding at a compound concentration of 1 μM.

Receptor	serotonin 5-HT$_{2C}$	serotonin 5-HT$_3$	dopaminergic D$_3$	adrenergic α$_1$	adrenergic α$_{2C}$	histamine H1	muscarinic M$_1$
% Inhibition	72	25	89	12	12	85	3

Crystal structure analysis of ligands

To obtain the protonated form of the synthesized compounds, several salts were considered. However, crystallization of the salts were unsuccessful. Good quality single crystals of free bases were obtained instead.

The crystal structures of two of the most potent 5-HT$_6$R ligands (**4** and **10**) revealed a similar hairpin-like conformation of the molecules, which differs from the bent conformation of the less active bioisosteres (**8** and **9**). The distinct orientation of the p-nitroaryl fragment and the second aromatic ring of the molecules is represented by the torsion angle C(2)-N(2)-C(11)-C(12) (Table 3). The hairpin conformation of **4** is a result of intramolecular hydrogen bond formation N(2)-H(2)...O(1) (Figure 2, Table 4), while in the case of **10** it is related to the conformation of the introduced seven-membered ring.

The hairpin conformation of the two most active bioisosteres allows the two aromatic fragments to be closer, which is reflected by centroids distance (Cg1-Cg2) of 5.1–5.5 Å. This conformation also results in a shorter distance between the basic nitrogen atom N(4) and the centroid (Cg2) of the aromatic ring C(12)-C(17), which varies between 6.8 to 7.7 Å for the most active ligands, whereas it is approximately 10 Å for the two less active compounds (Figure 2). Additionally, the close proximity of the C(12)-C(17) π-electron system influences the mutual orientation of both rings of the arylpiperazine moiety, which can be defined by the torsion angle C(3)-C(4)-N(3)-C(7). This angle for both active compounds is approximately ±30°. The opposite sign of this value is related to the opposite orientation of the aromatic C(12)-C(17) ring with respect to the piperazine ring. This distinct orientation is a result of the packing in the crystal structure. It is potentially based upon the formation of weak interaction C(13)-H(13)...O(2) in the crystal structure of **4**, which is not observed in **10**. For the latter structure, similar interactions occur between the

two methylene groups of the seven-membered ring and the oxygen atom O(1) as a bifurcated acceptor of weak hydrogen bond (see Table 4).

Within the crystal structure of the presented compounds, weak
5 hydrogen bonds C-H...O and C-H...N are primarily observed. The only exception is the crystal structure of **4**, in which the presence of the strong donor N(2) allowed centrosymmetric dimer formation through hydrogen bonding system (Table 3). The intramolecular interaction N(2)-H(2)...O(1) mentioned above
10 results in a co-planar arrangement of the nitro group with respect

to the aromatic ring C(1)-C(6). For compounds **8**, **9** and **10**, this co-planarity is not observed. The p-NO$_2$ substituent demonstrated different inductive effects in these molecules. The nitro group exhibits an electron withdrawing effect in **8** and **10** and a slightly
15 electron donating effect in **9**. The electron withdrawing effect is shown by the elongation of the N(1)-C(1) bond and the increased C(2)-C(1)-C(6) angle (Table 3). The differing properties of the nitro group are related to the number of intermolecular interactions in which the oxygen atoms are involved.
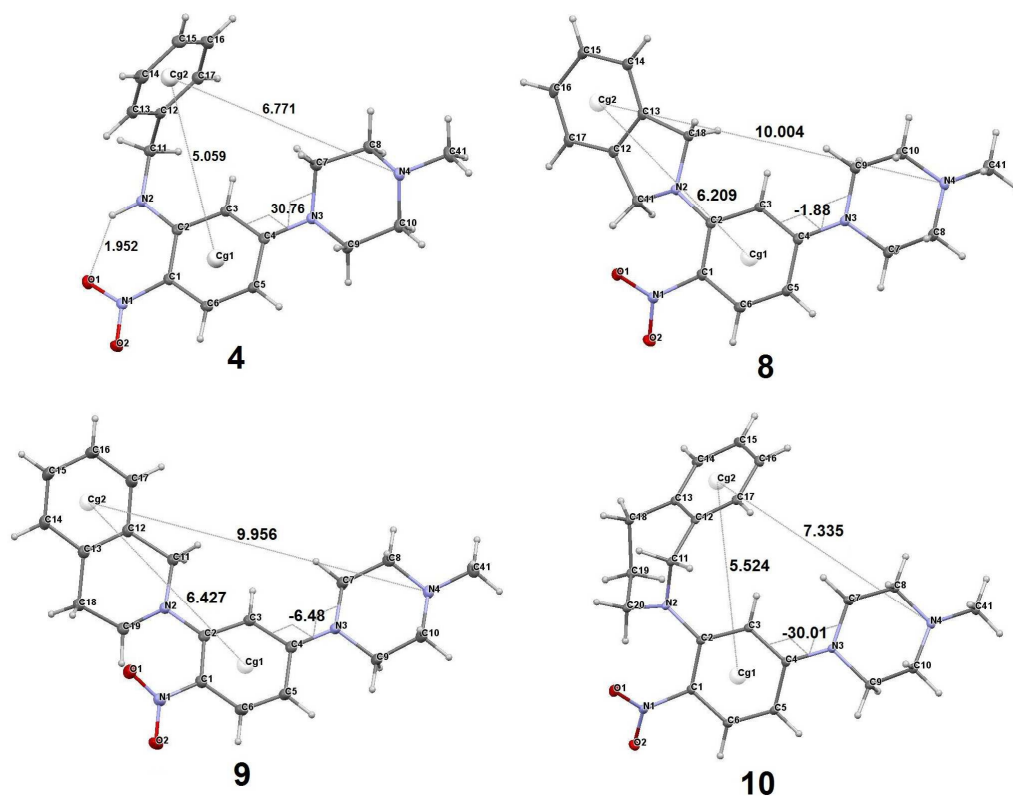

Figure 2 Molecular geometry and common geometrical features (distance in A and torsion angle value in °) that determine arrangement of molecules in the crystal environment. For **4**, an intramolecular hydrogen bond is highlighted. The displacement ellipsoids of the non-hydrogen atoms are drawn at the 30% probability level. H atoms are presented as small spheres with an arbitrary radius.

25 **Table 3** Selected geometrical values for the presented crystal structures [Å and °].

Compound	4	8	9	10
N(1)-C(1)	1.429(2)	1.443(1)	1.439(2)	1.444(1)
N(2)-C(2)	1.352(2)	1.380(1)	1.388(2)	1.380(1)
N(3)-C(4)	1.398(2)	1.385(1)	1.372(2)	1.385(1)
C(3)-C(4)-C(5)	118.5(1)	118.4(1)	116.6(1)	117.98(8)
C(2)-C(1)-C(6)	120.1(1)	121.0(1)	119.9(1)	121.00(8)
C(2)-N(2)-C(11)-C(12)	-69.1(2)	-173.34(9)	-165.0(1)	90.7(1)
O(1)-N(1)-C(1)-C(2)	4.0(2)	-36.9(2)	-22.6(2)	-33.5(1)
O(2)-N(1)-C(1)-C(6)	3.4(2)	-39.7(1)	-27.5(2)	-37.5(1)
C(3)-C(4)-N(3)-C(7)	30.76(2)	-1.9(2)	-6.5(2)	-30.01(1)
C(5)-C(4)-N(3)-C(9)	-8.5(2)	35.5(2)	21.3(2)	3.7(1)

ARTICLE TYPE

Table 4 Geometry of strong and weak hydrogen bonds in the crystal structures [Å and °].

Cmpd	D-H...A	d(D-H)	d(H...A)	d(D...A)	<(DHA)
4	N(2)-H(2)...O(1)	0.88(2)	1.95(2)	2.639(2)	133(2)
	N(2)-H(2)...O(1)_1	0.88(2)	2.31(2)	2.994(2)	134(1)
	C(10)-H(10A)...O(2)_2	0.99	2.52	3.419(2)	151
	C(13)-H(13)...O(2)_3	0.95	2.56	3.505(2)	175
8	C(11)-H(11A)...O(1)	0.99	2.12	2.870(1)	130
	C(11)-H(11A)...N(1)	0.99	2.52	3.051(2)	113
	C(7)-H(7A)...O(1)_4	0.99	2.57	3.301(1)	130
	C(9)-H(9B)...O(2)_5	0.99	2.59	3.537(2)	161
	C(5)-H(5)...O(2)_5	0.95	2.61	3.549(1)	171
9	C(11)-H(11B)...N(4)_6	0.99	2.61)	3.293(2)	126
	C(18)-H(18B)...O(1)	0.99	2.55	3.164(2)	120
	C(19)-H(19A)...N(1)	0.99	2.47	3.124(2)	123
10	C(11)-H(11B)...O(1)_7	0.99	2.49	3.437(1)	161
	C(18)-H(18B)...O(1)_7	0.99	2.48	3.419(1)	159
	C(20)-H(20B)...N(1)	0.99	2.35	3.004(1)	123

Symmetry transformations used to generate equivalent atoms: _1: -x,-y,-z; _2: -x,y+1/2,-z+1/2; _3: -x,1-y,-z; _4: x-1,y,z; _5: x,-y+3/2,z+1/2 _6: ;-x,y-1/2,-z+1/2; _7: -x+1,-y+1,-z+1

Docking studies

Compounds **4**, **8**, **9** and **10** were ionized and docked without any restraints to 200 homology models of 5-HT$_6$R (aligned on an β2-adrenergic template) developed in our laboratory employing a previously utilized approach (see experimental).[14,28,29] For each compound, only the best docking pose per receptor was considered, and the 100 best scoring complexes were transformed into bitstrings by applying SIFt formalism to statistically describe the interactions between ligand and receptor.[30,31] The most potent compounds **4** and **10** (Figure 3A, D) were classically docked near TM3 and TM5. Crucial charge-reinforced hydrogen bonds of protonated nitrogen were formed with D3.32, and hydrophobic interactions were created with W3.28, T3.29 and C3.36. The methyl group of the N-methyl-arylpiperazine also interacted with TM7 (Y7.43). The central nitrophenyl group directed toward TM6 participated in edge-to-face contacts with F6.51 and F6.52. In case of compound **4**, the benzyl moiety was near EL2 and participated in a hydrophobic interaction with L164. On the other hand, benzazepine moiety of **10** was situated deep into the subpocket near TM5 and interacted with F5.38, A5.42, S5.43 (statistically, the most important TM5 residue) and T5.46. Surprisingly, both of the less potent compounds (**8** and **9**) formed hydrogen bonds between the positive, ionized nitrogen atom and D7.36 (instead of D3.32). Thus, they were located shallowly in the binding pocket, close to TM6 and TM7; consequently, these compounds had almost no interaction with TM3 (Figure 3B, C). The central nitrophenyl group did not contact F6.52, but participated in face-to-edge stacking with F6.51 and strongly interacted with EL2 (especially L164). Despite the fact that the side phenyl moiety was positioned toward TM5 deeper into the receptor, it did not interact with S5.43 and T5.46.

RSC Advances

Cite this: DOI: 10.1039/c0xx00000x

www.rsc.org/xxxxxx

ARTICLE TYPE
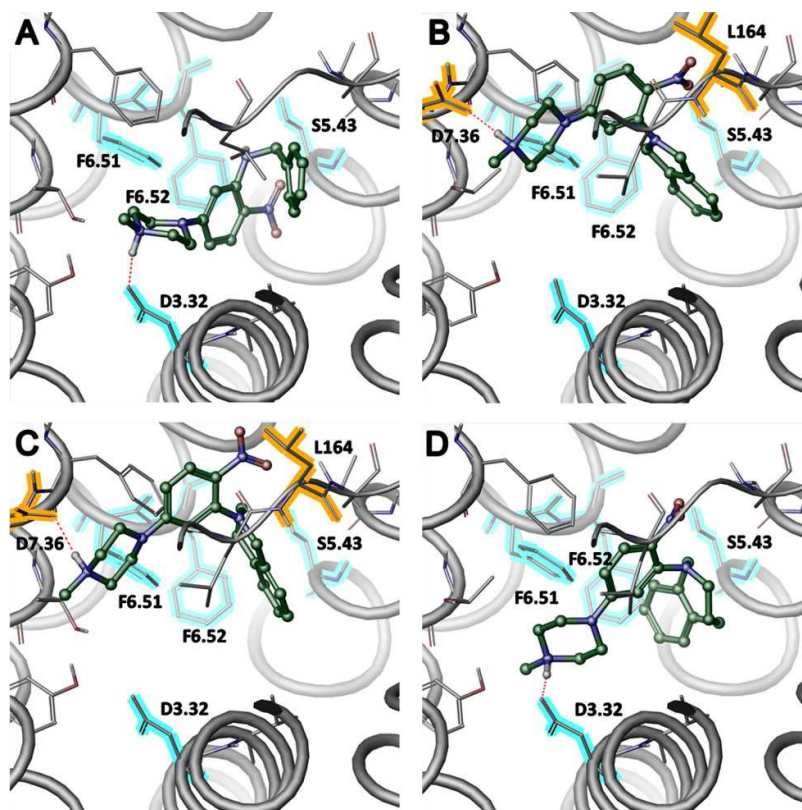
Figure 3. Computational models of the best scoring complexes between ligand **4** (A), **8** (B), **9** (C), **10** (D) and 5-HT$_6$R. The important residues that are statistically crucial for the more potent ligands are marked in cyan. Residues (D7.36 and L164) that interact with the less active compounds are indicated in orange. Hydrogen bonds with D3.32 or D7.36 are shown in red. Both **4** and **10** are situated deeper into the receptor cavity and strongly interact with
5 TM3, TM5 and TM6, whereas the less potent **8** and **9** are located shallowly and interact with TM7 and EL2.

Table 5 Averaged SIFt profiles calculated for the100 best scoring complexes. Only values higher than 0.50 were selected as significant.

Residue	Compound			
	4	**8**	**9**	**10**
W3.28	0.79	–	–	0.74
T3.29	0.61	0.56	–	0.64
D3.32	**0.99**	–	–	**0.98**
V3.33	0.85	0.79	0.84	**0.96**
C3.36	0.88	–	–	**0.90**
L4.61	–	0.51	–	–
R162	–	–	0.57	–
L163	**0.98**	**0.96**	**0.98**	**0.99**
L164	0.59	0.60	0.64	–
A165	0.87	0.83	0.86	**0.98**
F5.38	0.63	0.89	0.82	**0.99**
V5.39	**1.00**	**0.93**	0.82	**0.99**
A5.42	0.65	0.76	0.68	**0.95**
S5.43	**0.95**	–	–	0.72
T5.46	0.63	–	–	0.85
F6.51	**1.00**	**0.96**	**0.95**	**1.00**
F6.52	**0.98**	–	0.56	**0.99**
N6.55	**0.99**	0.86	0.86	**1.00**
V6.58	0.67	–	0.58	0.50
P7.32	–	–	0.50	–
F7.35	**0.99**	**0.99**	**1.00**	**1.00**
D7.36	–	0.58	0.77	–
T7.39	**1.00**	0.74	0.75	**1.00**
Y7.43	**0.94**	0.54	–	**0.93**

Discussion

Common VS campaigns use the structures of active compounds as direct queries to search databases; however, here, we introduced an additional step of bioisostere generation to cover more biologically relevant chemical space. Indeed, the similarity between the 11 VS hits and the 5-HT$_6$R ligand database ranged from Tc = 0.57–0.83. Particularly, Tc equaled 0.79 for the hit compound (**9**), which means that this compound would not have been selected using a standard VS procedure with the criteria of Tc $\geq$ 0.8. Further bioisosteric modification of **9** based on ring alteration produced two additional compounds with significantly different affinities for 5-HT$_6$R (K_i = 245 and 6 nM for **8** and **10**, respectively). The parent compound N-benzyl-5-(4-methylpiperazin-1-yl)-2-nitroaniline **4** was previously reported by Tasler et al. in a series of 5-HT$_6$R ligands developed by modifying virtual screening hits.[25] The most potent compound of a group of obtained nitrophenylpiperazines displayed affinity K_i = 6 nM towards 5-HT$_6$R.

Crystallographic studies of synthesized bioisosteres revealed that both compounds with higher binding affinities (**4** and **10**) adopt a similar molecular arrangement. The mutual orientation of both aromatic moieties, and consequently, the shorter distance between the C(12)-C(17) ring and the basic nitrogen atom N(4) seems to play an important role. Interestingly, the binding poses of the docked ligands resemble crystalline structures. Distances between the aromatic rings are 1 Å greater, on average, in less potent compounds than in compounds **4** and **10**, similar to the intervals between the N(4) atoms of the N-methylpiperazine moiety and the terminal aromatic system. These substructures are relatively distant for compounds **8** and **9**, whereas in the

structures **4** and **10**, the distance values are decreased by 2-3 Å. Similar orientations of the rings in the arylpiperazine fragment for both of the more active compounds may be critical for ligand-receptor recognition and may play an important role in selective ligand-receptor binding. The semi-rigid molecule **10** represents optimal spatial orientation of the crucial molecular fragments, thus allowing more precise definition of the pharmacophore. The same conformation is also possible for the most flexible molecule **4**, although this was not observed in the crystalline form because of the additional interactions formed in the crystal lattice. This favorable conformation cannot be attained by **8** and **9** because of their increased rigidity, which explains the lower binding affinity of these compounds for the 5-HT$_6$ receptor.

The statistical analysis of multiple ligand-receptor complexes (Table 5) emphasizes the importance of L163, F6.51 and F7.35 in ligand binding. In addition, the more potent compounds, **4** and **10**, interacted classically with D3.32, S5.43, T5.46 and F6.52, whereas the binding modes of the rigid, less potent compounds **8** and **9** indicated atypical interactions with D7.36 (instead of D3.32). Interestingly, of the entire serotonin GPCR family of 13 receptors, the D7.36 residue is present only in 5-HT$_{1B}$ and 5-HT$_{1D}$ receptors. As far as we know, this alternative side interaction of a protonated nitrogen with D7.36 has not been previously reported. This information can be used as a potential starting point for the design of novel, potent, selective serotonin receptor ligands.

Conclusion

In conclusion, bioisosteric exchange based on ring modification was successfully applied to the design of potent 5-HT$_6$R ligands with a modified selectivity profile. Whereas a rigid conformation between two aromatic moieties in compounds **8** and **9** resulted in decreased affinity, the introduction of a seven-membered ring in compound **10** conserved the active spatial orientation of the important pharmacophore features. These observations were confirmed and explained by crystallographic and computational studies. Compared to the previously reported compound **4**, the most potent compound **10** exhibited greater selectivity towards 5-HT$_{1A}$ (three-fold), 5-HT$_7$ (seven-fold) and D$_2$ (two-fold). These differences in biological activity suggest that 5-HT$_6$ receptors are sensitive to subtle changes in the orientation of the aromatic moieties. Additionally, analysis of the ligand-receptor complexes indicated the possibility of the formation of an unusual interaction with D7.36, which has not been previously reported.

Experimental protocols

Synthesis

Melting points were determined on an Electrothermal 9100. ^{1}H NMR spectra were recorded on Bruker Avance III HD 400 NMR spectrometer. Mass spectra were recorded using a TQD Waters LC/MS spectrometer with electrospray ionization. Substrates and solvents were purchased from Sigma-Aldrich and Apollo Scientific and were used without further purification.

N-Benzyl-5-chloro-2-nitroaniline (1).
5-Chloro-2-nitroaniline (1.0 g) was added to water (12.0 ml), benzyl bromide (1.19 g) was added, and the reaction was heated to reflux for 1.5 h. After cooling to RT, a saturated sodium

RSC Advances Accepted Manuscript

bicarbonate solution (10.0 ml) was added to the reaction mixture, and the product was extracted 3 times with ethyl acetate (3×20 ml). The combined extracts were washed with brine, dried over anhydrous $MgSO_4$ and evaporated under reduced pressure. Purification by column chromatography on silica eluting with chloroform/hexane 1:1 afforded a yellow solid (0.71 g). Yield 45%.

LCMS [M+1] = 263.09 m/z (262.05 calcd). ^{1}H NMR (CDCl$_3$, 400.17 MHz) δ (ppm): 4.54 (d, J = 5.5 Hz, 2H); 6.66 (dd, J = 9.1, 2.1 Hz, 1H); 6.86 (d, J = 2.1 Hz, 1H); 7.48 – 7.27 (m, 5H); 8.22 – 8.12 (m, 1H); 8.47 (d, J = 6.1 Hz, 1H).

^{13}C NMR (CDCl$_3$, 400.17 MHz) δ (ppm): 47.27; 113.60; 116.32; 127.17; 127.99; 128.27; 129.07; 130.89; 136.9; 142.86; 145.62.

tert-Butyl N-benzyl-N-(5-chloro-2-nitrophenyl)carbamate (2).

N-Benzyl-5-chloro-2-nitroaniline (1) (0.66 g) was dissolved in anhydrous THF (10 ml), and the solution was cooled in an ice bath. Then, a 0.5 M solution (5.82 ml) of KHMDS in toluene was added dropwise. After standing for 30 min, a solution of Boc$_2$O (0.64 g) in anhydrous THF (10 ml) was added dropwise. The reaction mixture was allowed to warm to RT and was stirred until completion (as indicated by TLC). The reaction was quenched by the addition of distilled water (50 ml), and the product was extracted with chloroform. Purification by column chromatography on silica eluting with chloroform afforded a red solid (0.35 g). Yield 40%. The substance could not be ionized under ESI conditions. ^{1}H NMR (CDCl$_3$, 400.17 MHz) δ (ppm): 1.56 (s, 9H); 4.54 (d, J = 5.5 Hz, 2H); 6.66 (dd, J = 9.1, 2.1 Hz, 1H); 6.86 (d, J = 2.1 Hz, 1H); 7.48 – 7.29 (m, 5H); 8.17 (dd, J = 9.1, 0.3 Hz, 1H).

^{13}C NMR (CDCl$_3$, 400.17 MHz) δ (ppm): 27.43; 47.27; 85.17; 113.60; 116.32; 127.16; 127.98; 128.27; 129.07; 136.58; 142.85; 145.62; 146.75.

General procedure for the coupling of 4-chloro-2-fluoro-1-nitrobenzene with heterocyclic secondary amines.

4-Chloro-2-fluoro-1-nitrobenzene (5.7 mmol) and the appropriate amine (5.7 mmol) were dissolved in DMSO (10 ml), and anhydrous potassium carbonate (14.2 mmol) was added. The reaction mixture was heated to 120 °C for 2 h. After cooling to RT, the reaction mixture was poured into distilled water (100 ml) and extracted with ethyl acetate (3×30 ml). The combined extracts were washed with distilled water (2×100 ml) and brine (20 ml), dried over anhydrous $MgSO_4$ and evaporated under reduced pressure. Purification was performed by flash chromatography on silica gel eluting with chloroform.

2-(5-Chloro-2-nitrophenyl)-2,3-dihydro-1H-isoindole (5).

A red solid was obtained (1.2 g). Yield 76%. LCMS [M+1] = 275.05 m/z (274.05 calcd). ^{1}H NMR (CDCl$_3$, 400.17 MHz) δ (ppm): 4.68 (s, 4H); 6.77 (dd, J = 8.7, 2.0 Hz); 7.03 (d, J = 2.0 Hz); 7.40 – 7.25 (m, 4H); 7.67 (d, J = 8.7 Hz).

^{13}C NMR (CDCl$_3$, 400.17 MHz) δ (ppm): 55.67, 116.00, 116.38, 122.25, 127.72, 127.84; 135.95; 136.36; 139.02; 142.07.

2-(5-Chloro-2-nitrophenyl)-1,2,3,4-tetrahydroisoquinoline (6).

A red solid was obtained (1.34 g). Yield 82%. LCMS [M+1] = 289.06 m/z (288.06 calcd). ^{1}H NMR (CDCl$_3$, 400.17 MHz) δ (ppm): 3,05 (t, 2H); 3.43 (t, J = 6.2, 5.4 Hz, 2H); 4,32 (s, 2H); 6.92 (dd, J = 8.7, 2.1 Hz, 1H); 7.15 – 7.08 (m, 1H); 7.30 – 7.15 (m, 4H); 7.82 (d, J = 8.7 Hz, 1H). 13C NMR (CDCl3, 400.17 MHz) δ (ppm): 28.72; 49.78; 52.12; 119.12; 119.58; 126.30;

126.32; 126.87; 128.07; 128.71; 133.17; 134.37; 138.89; 139.78; 146.34.

2-(5-Chloro-2-nitrophenyl)-2,3,4,5-tetrahydro-1H-2-benzazepine (7).

A red solid was obtained (0.32 g). Yield 18%. LCMS [M+1] = 303.08 m/z (302.08 calcd). ^{1}H NMR (CDCl$_3$, 400.17 MHz) δ (ppm): 2.09 – 1.98 (m, 2H; 2.99 – 2.92 (m, 2H); 3.45 – 3.37 (m, 2H); 4.50 (s, 2H); 6.76 (dd, J = 8.7, 2.1 Hz, 1H); 7.03 (d, J = 2.1 Hz, 1H); 7.31 – 7.12 (m, 4H); 7.67 (d, J = 8.7 Hz, 1H).

^{13}C NMR (CDCl$_3$, 400.17 MHz) δ (ppm): 27.53; 33.72; 55.49; 56.65; 118.37; 119.45; 126.68; 127.78; 127.82; 128.22; 129.83; 137.36; 137.97; 139.18; 140.85; 146.21.

General procedure for the coupling of N-Me-piperazine with aryl chloride.

An oven-dried round-bottom flask was charged with the aryl chloride (3.6 mmol), palladium acetate (0.1 eq.), biphenyl tert-butyl phosphine (JohnPhos) (0.2 eq.) and potassium phosphate monohydrate (1.4 eq.). The flask was evacuated under vacuum and filled with argon three times. Then, DME (2 ml / 1 mmol) and N-methylpiperazine (1.3 eq.) were added via syringe. The reaction mixture was heated at 100 °C for 20 h. After completion, the reaction mixture was filtered through celite, and the solvent was evaporated. The product was purified by column chromatography on silica eluting with CHCl$_3$:MeOH (19:1)

N-Benzyl-5-(4-methylpiperazin-1-yl)-2-nitroaniline (4).

A red oil was obtained (0.21 g). Yield 51%. LCMS [M+1] = 327.24 m/z (426.23 calcd); the compound undergoes deprotection during ionization. tert-Butyl N-benzyl-N-[5-(4-methylpiperazin-1-yl)-2-nitrophenyl]carbamate (3) (0.20 g) was dissolved in MeOH (10 ml) with a few drops of concentrated hydrochloric acid. The reaction was heated to reflux for 3 h, and distilled water (50 ml) and 15% NaOH solution (5 ml) were added. The products were extracted with chloroform (3×20 ml), and the extracts were dried over anhydrous $MgSO_4$ and evaporated under reduced pressure. The obtained substance was dissolved in diethyl ether and converted to the hydrochloride salt by addition of a 20% solution of HCl in diethyl ether. The collected solids were recrystallized from ethanol to afford an orange solid (0.094 g). Yield 55%.

For the purpose of crystallographic studies, the free base was crystallized from hexane/acetone.

Hydrochloride mp. 206-208 °C. LCMS [M+1] = 327.17 m/z (326.17 calcd). ^{1}H NMR (CDCl$_3$, 400.17 MHz) δ (ppm): 2.31 (s, 3H), 2.47 – 2.42 (m, 4H), 3.32 – 3.27 (m, 4H), 4.50 (d, J = 5.4 Hz, 2H), 5.84 (d, J = 2.6 Hz, 1H), 6.22 (dd, J = 9.7, 2.6 Hz, 1H), 7.33 – 7.24 (m, 1H), 7.39 – 7.30 (m, 4H), 8.08 (d, J = 9.7 Hz, 1H), 8.79 (t, J = 5.5 Hz, 1H).

^{13}C NMR (CDCl$_3$, 400.17 MHz) δ (ppm): 46.02; 46.80; 47.08; 47.20; 54.48; 94.42; 104.48; 124.46; 127.12; 127.59; 128.88; 128.94; 137.62; 147.44; 155.73.

2-[5-(4-Methylpiperazin-1-yl)-2-nitrophenyl]-2,3-dihydro-1H-isoindole (8).

An orange solid was obtained (0.5 g). Hydrochloride mp. 208-210 °C. LCMS [M+1] = 339.17 m/z (338.17 calcd). ^{1}H NMR (CDCl$_3$, 400.17 MHz) δ (ppm): 2.39 (s, 3H); 2.66 – 2.55 (m, 4H); 3.47 – 3.37 (m, 4H); 4.68 (s, 4H); 6.26 (d, J = 2.5 Hz, 1H); 6.36 (dd, J = 9.3, 2.4 Hz, 1H); 7.30 (s, 4H); 7.83 (d, J = 9.3 Hz, 1H).

^{13}C NMR (CDCl$_3$, 400.17 MHz) δ (ppm): 45.92; 47.37; 54.56;

55.90; 99.52; 104.47; 122.14; 127.40; 129.39; 130.17; 136.62; 144.46; 154.51.

2-[5-(4-Methylpiperazin-1-yl)-2-nitrophenyl]-1,2,3,4-tetrahydroisoquinoline (9).

An orange solid was obtained (0.7 g). Hydrochloride mp. 157-159 °C. LCMS [M+1] = 353.17 m/z (352.19 calcd). ^{1}H NMR (CDCl$_3$, 400.17 MHz) δ (ppm): 2.39 (s, 3H); 2.62 – 2.55 (m, 4H); 3.10 (t, J = 5.8 Hz, 2H); 3.41 (ddd, J = 7.7, 5.5, 4.5 Hz, 6H); 4.34 (d, J = 1.0 Hz, 2H); 6.50 – 6.40 (m, 2H); 7.26 – 7.07 (m, 4H); 8.10 – 8.00 (m, 1H).

^{13}C NMR (CDCl$_3$, 400.17 MHz) δ (ppm): 28.92; 46.04; 47.15; 50.89; 52.56; 54.60; 102.64; 106.33; 125.96; 126.27; 126.56; 128.83; 129.91; 131.54; 133.92; 134.75; 148.97; 154.92.

2-[5-(4-Methylpiperazin-1-yl)-2-nitrophenyl]-2,3,4,5-tetrahydro-1H-2-benzazepine (10).

An orange solid was obtained (0.8 g). Hydrochloride mp. 136-138 °C. LCMS [M+1] = 367.22 m/z (366.20 calcd). ^{1}H NMR (CDCl$_3$, 400.17 MHz) δ (ppm): 2.05 – 1.94 (m, 2H); 2.33 (s, 3H); 2.51 – 2.42 (m, 4H); 2.99 – 2.89 (m, 2H); 3.23 – 3.16 (m, 4H); 3.45 – 3.36 (m, 2H); 4.57 (s, 2H); 6.35 – 6.24 (m, 2H); 7.32 – 7.09 (m, 4H); 7.87 (dd, J = 9.0, 0.5 Hz, 1H).

^{13}C NMR (CDCl$_3$, 400.17 MHz) δ (ppm): 28.00; 34.06; 45.94; 47.03; 47.17; 54.44; 54.52; 56.59; 56.68; 103.08; 105.43; 126.26; 126.30; 127.41; 128.01; 129.49; 129.99; 130.39; 139.12; 141.23; 148.76; 154.43.

X-ray structure determination

Single crystals of all compounds were obtained from a 1:1 acetone:hexane mixture by slow evaporation of the solvent under ambient conditions. X-ray diffraction data for crystals of **4**, **8** and **10** were collected with MoKα radiation (λ=0.71073 Å) using a Nonius Brucker KappaCCD diffractometer with the software COLLECT.[32] Data were processed with HKL_SCALEPACK and HKL_DENZO.[33] For the selected crystal **9,** intensities of the diffracted X-ray beam were collected with CuKα radiation (λ=1.54184 Å) using SuperNova diffractometer. Data were processed with CrysAlisPro.[34] Experiments were performed at 100(2) K for all compounds except **9**. For **9**, the temperature was set at 110(2) K. The phase problem was solved by direct methods with SHELXS-97 program. The model parameters were refined by full-matrix least-squares on F^2 using SHELXL-97.[35] All non-hydrogen atoms were refined anisotropically. In the structure of **4**, the hydrogen atom attached to N2 was localized on the difference Fourier map and refined without restraints. For all compounds, the positions of the hydrogen atoms attached to C atoms were constrained with C-H = 0.95 Å for aromatic protons, C-H = 0.99 Å for methylene protons, and C-H = 0.98 Å for methyl groups and were refined using the riding model with the isotropic displacement parameter U$_{iso}$ = 1.2 U$_{eq}$ and U$_{iso}$ = 1.5 U$_{eq}$ (methyl groups only) of the parent atom.

All crystallographic data for the presented structures are shown in Table 6.

Unit cell layout is presented in Supplementary Infromation Figures

WinGX software was used to prepare the materials for publication.[36] The figures showing the asymmetric units of the structures were obtained using Mercury CSD 3.3.[37]

Table 6 Crystal data and structure refinement.

Identification code	**4**	**8**	**9**	**10**
Molecular formula	$C_{18}H_{22}N_4O_2$	$C_{19}H_{22}N_4O_2$	$C_{20}H_{24}N_4O_2$	$C_{21}H_{26}N_4O_2$
Formula weight	326.39	338.40	352.43	366.46
Wavelength	0.71073 Å	0.71073 Å	1.54184 Å	0.71073 Å
Crystal system	Monoclinic	Monoclinic	Monoclinic	Triclinic
Space group	P 2_1/c	P 2_1/c	P 2_1/c	P $\overline{1}$
Unit cell dimensions	a = 14.8320(4) Å b = 4.8941(2) Å c = 23.9340(7) Å β = 108.015(2)°	a = 9.2516(3) Å b = 18.4177(5) Å c = 12.6426(3) Å β = 128.998(2)°	a = 14.6428(3) Å b = 7.5669(1) Å c = 16.1976(3) Å β = 100.828(2)°	a = 9.5413(2) Å b = 10.1771(2) Å c = 11.0759(2) Å α = 105.049(2)° β = 92.969 (2)° γ = 114.710 (1)°
Volume [Å^3]	1652.15(10)	1674.18(9)	1762.75(6)	927.62(3)
Z	4	4	4	2
Dcalc [g/cm^3]	1.312	1.343	1.328	1.312
Absorption coefficient [mm^{-1}]	0.088	0.090	0.707	0.086
F(000)	696	720	752	392
Crystal size [mm^3]	0.50 x 0.30 x 0.05	0.50 x 0.40 x 0.20	0.35 x 0.25 x 0.05	0.50 x 0.50 x 0.30
θ range [°]	2.62 - 28.68	2.35 - 27.50	3.07 - 71.24	2.79 - 27.45
Index ranges	-19<=h<=19, -6<=k<=4, -32<=l<=32	-11<=h<=12, -21<=k<=23, -15<=l<=16	-17<=h<=17, -9<=k<=9, -19<=l<=18	-12<=h<=11, -12<=k<=13, -14<=l<=14
Reflections collected	10299	9948	23634	7289
Independent reflections	4234 [R$_{(int)}$= 0.0329]	3819 [R$_{(int)}$= 0.0185]	3397 [R$_{(int)}$= 0.0483]	4191 [R$_{(int)}$= 0.0107]
Completeness %	99.6 (to θ=25.24°)	99.5 (to θ=25.24°)	100.0 (to θ=67.68°)	99.4 (to θ=25.24°)
Data/restraints/parameters	4234 / 0 / 221	3819 / 0 / 226	3397 / 2 / 235	4191 / 0 / 244
Goodness-of-fit on F^2	1.016	1.038	1.021	1.027
Final R indices [I>2σ(I)]	R1 = 0.0469, wR2 = 0.1076	R1 = 0.0378, wR2 = 0.0949	R1 = 0.0385, wR2 = 0.0977	R1 = 0.0352, wR2 = 0.0938
R indices (all data)	R1 = 0.0736, wR2 = 0.1199	R1 = 0.0444, wR2 = 0.0993	R1 = 0.0465, wR2 = 0.1051	R1 = 0.0376, wR2 = 0.0961
Δρ$_{max}$/Δρ$_{min}$ [e.Å^{-3}]	0.243/ -0.292	0.321/ -0.268	0.200/ -0.211	0.298/ -0.245

In vitro pharmacology

Cell culture and preparation of cell membranes

HEK293 cells with stable expression of human serotonin 5-HT$_{1A}$R, 5-HT$_6$, 5-HT$_{7b}$R or dopamine D$_{2L}$R (prepared with the use of Lipofectamine 2000) were maintained at 37 °C in a humidified atmosphere with 5% CO$_2$ and were grown in Dulbecco's Modifier Eagle Medium containing 10% dialyzed fetal bovine serum and 500 µg/ml G418 sulfate. For membrane preparations, cells were subcultured in 10 cm diameter dishes, grown to 90% confluence, washed twice with phosphate buffered saline (PBS), pre-warmed to 37 °C and pelleted by centrifugation (200 g) in PBS containing 0.1 mM EDTA and 1 mM dithiothreitol. Prior to membrane preparations, the pellets were stored at –80 °C.

Radioligand binding assays

Cell pellets were thawed and homogenized in 20 volumes of assay buffer using an Ultra Turrax tissue homogenizer and centrifuged twice at 35000 g for 20 min at 4 °C, with incubation for 15 min at 37 °C in between rounds of centrifugation. The composition of the assay buffers was as follows: for 5-HT$_{1A}$R: 50 mM Tris–HCl, 0.1 mM EDTA, 4 mM MgCl$_2$, 10 µM pargyline and, 0.1% ascorbate; for 5-HT$_6$R: 50 mM Tris–HCl, 0.5 mM EDTA and 4 mM MgCl$_2$, for 5-HT$_{7b}$R: 50 mM Tris–HCl, 4 mM MgCl$_2$, 10 µM pargyline and 0.1% ascorbate; for dopamine D$_{2L}$R: 50 mM Tris–HCl, 1 mM EDTA, 4 mM MgCl$_2$, 120 mM NaCl, 5 mM KCl, 1.5 mM CaCl$_2$ and 0.1% ascorbate.

All assays were incubated in a total volume of 200 µl in 96-well microliter plates for 1 h at 37 °C, except for 5-HT$_{1A}$R, which was incubated at room temperature for 1 h. The process of equilibration was terminated by rapid filtration through Unifilter plates with a 96-well cell harvester, and the radioactivity retained on the filters was quantified on a Microbeta plate reader.

For displacement studies, the assay samples contained the following as radioligands: 1.5 nM [³H]-8-OH-DPAT (187 Ci/mmol) for 5-HT$_{1A}$R; 2 nM [³H]-LSD (85.2 Ci/mmol for 5-HT$_6$R; 0.6 nM [³H]-5-CT (39.2 Ci/mmol) for 5-HT$_{7b}$R or [³H]-Raclopride (74.4 Ci/mmol).

Non-specific binding was defined with 10 µM of 5-HT in 5-HT$_{1A}$R and 5-HT$_{7b}$R binding experiments, whereas 10 µM methiothepine and 1 µM of (+)butaclamol were used in the 5-HT$_6$R and D$_{2L}$ assays, respectively. Each compound was tested in triplicate at 7 to 8 different concentrations (10^{-11}–10^{-4} M). The inhibition constants (K_i) were calculated from the Cheng-Prusoff equation [27]. The results are expressed as the means of at least two separate experiments.

Initial screening experiments were performed using the same conditions with two compound concentrations: 10^{-6} and 10^{-7} M.

Molecular modeling

Preparation of ChEMBL database

Due to a large diversity of activity measures, only the compounds with defined K_i (IC_{50} − assumed as $2\times K_i$, pK_i or pIC_{50} were converted to K_i), as assayed on human cloned receptors or on rat cloned or native receptors, were considered. In case there were multiple data for one ligand, the K_i and human receptors were given preference; a median value was used if there were many biological results.

Compounds preparation

The appropriate ionization states at pH=7.4 for all structures used in screening and docking procedures were assigned using Epik [28]. 3D structures were generated in Ligprep under default settings (force field used OPLS2005, retention of specified chiralities and generation of only one low energy ring conformation per ligand).

ADME filters

The following criteria were used to filter compounds with unfavorable profiles: the number of reactive functional groups (desirable range of values: 0-2), logarithm of calculated aqueous solubility (−6.5-0.5 mole/liter), gut-blood barrier (>500 nm/s) and blood-brain barrier penetration coefficient (−3.0-1.2).

Docking protocol

All receptors were centered at D3.32 with the grid box size set to $25\times25\times25$ Å. Docking runs were performed in Glide software at the SP level under default settings (sampling nitrogen inversion, sampling ring conformations with energy window equal to 2.5 kcal/mol, penalizing nonplanar conformation of amides up to 100 steps during energy minimization and performing post-docking optimization).

Supplementary Materials

Table showing structure of 11 selected and purchased compounds from virtual screening procedure and NMR spectra for synthesized compounds are available free of charge via the Internet. Crystallographic data (excluding structure factors) for the structures in this paper have been deposited with the Cambridge Crystallographic Data Centre as supplementary publication nos. CCDC 995671 (**4**), CCDC 995672 (**8**), CCDC 995673 (**9**) and CCDC 995674 (**10**). Copies of the data can be obtained, free of charge, by application to CCDC, 12 Union Road, Cambridge CB2 1EZ, UK, (fax: +44-(0)1223-336033 or e-mail: deposit@ccdc.cam.ac.uk).

Acknowledgements

Notes and references

† Electronic Supplementary Information (ESI) available: See DOI: 10.1039/b000000x/

1   L. M. Lima and E. J. Barreiro, *Curr. Med. Chem.*, 2005, **12**, 23–49.
2   G. Domagk, *DMW - Dtsch. Medizinische Wochenschrift*, 1935, **61**, 250–253.
3   P. Fludzinski, D. A. Evrard, W. E. Bloomquist, W. B. Lacefield, W. Pfeifer, N. D. Jones, J. B. Deeter and M. L. Cohen, *J. Med. Chem.*, 1987, **30**, 1535–1537.
4   Z. Tomaszewski, M. P. Johnson, X. Huang and D. E. Nichols, *J. Med. Chem.*, 1992, **35**, 2061–2064.
5   B. M. Mathes, K. J. Hudziak, J. M. Schaus, Y.-C. Xu, D. L. Nelson, D. B. Wainscott, S. E. Nutter, W. H. Gough, T. A. Branchek, J. M. Zgombick and S. A. Filla, *Bioorg. Med. Chem. Lett.*, 2004, **14**, 167–70.
6   M. Skultety, H. Hübner, S. Löber and P. Gmeiner, *J. Med. Chem.*, 2010, **53**, 7219–7228.
7   A. Burger, *Medicinal Chemistry, 3 rd Ed., NY, EUA, Wiley,* 1970.
8   A. V Ivachtchenko, Y. A. Ivanenkov and A. V Skorenko, *Expert Opin. Ther. Pat.*, 2012, **22**, 1123–68.
9   G. Rossé and H. Schaffhauser, *Curr. Top. Med. Chem.*, 2010, **10**, 207–21.
10 W. J. Geldenhuys and C. J. Van der Schyf, *Expert Rev. Neurother.*, 2009, **9**, 1073–85.
11 A. Quiedeville, M. Boulouard, V. Da Silva Costa-Aze, F. Dauphin, V. Bouet and T. Freret, *Rev. Neurosci.*, 2014, **25**, 417–27.
12 D. Heal, J. Gosden and S. Smith, *Int. Rev. Neurobiol.*, 2011, **96**, 73–109.
13 A. S. Garfield, L. K. Burke, J. Shaw, M. L. Evans and L. K. Heisler, *Behav. Brain Res.*, 2014, **266**, 1–6.
14 K. Rataj, J. Witek, S. Mordalski, T. Kosciolek and A. J. Bojarski, *J. Chem. Inf. Model.*, 2014, **54**, 1661–1668.
15 R. Kurczab, M. Nowak, Z. Chilmonczyk, I. Sylte and A. J. Bojarski, *Bioorg. Med. Chem. Lett.*, 2010, **20**, 2465–2468.
16 M. Kołaczkowski, M. Nowak, M. Pawłowski and A. J. Bojarski, *J. Med. Chem.*, 2006, **49**, 6732–6741.
17 D. Warszycki, S. Mordalski, K. Kristiansen, R. Kafel, I. Sylte, Z. Chilmonczyk and A. J. Bojarski, *PLoS One*, 2013, **8**, e84510.
18 R. Kurczab and A. J. Bojarski, *J. Chem. Inf. Model.*, 2013, **53**, 3233–43.
19 A. Gaulton, L. J. Bellis, A. P. Bento, J. Chambers, M. Davies, A. Hersey, Y. Light, S. McGlinchey, D. Michalovich, B. Al-Lazikani and J. P. Overington, *Nucleic Acids Res.*, 2012, **40**, D1100–D1107.
20 W. A. Warr, *J. Comput. Aided. Mol. Des.*, 2012, **26**, 801–804.
21 P. Zajdel, R. Kurczab, K. Grychowska, G. Satała, M. Pawłowski and A. J. Bojarski, *Eur. J. Med. Chem.*, 2012, **56**, 348–60.
22. Calculator Plugins Were Used for Structure Property Prediction and Calculation, Marvin 6.2.2, 2014, ChemAxon (http://www.chemaxon.com).
23. Schrödinger Release 2014-1: LigPrep, Version 2.9, Schrödinger, LLC, New York, NY, 2014.
24. Small-Molecule Drug Discovery Suite 2014-1: QikProp, Version 3.9, Schrödinger, LLC, New York, NY, 2014.
25 S. Tasler, J. Mies and M. Lang, *Adv. Synth. Catal.*, 2007, **349**, 2286–2300.
26. Marvin Was Used for Drawing, Displaying and Characterizing Chemical Structures, Substructures and Reactions, Marvin 6.2.2, 2014, ChemAxon (http://www.chemaxon.com).
27 C. Yung-Chi and W. H. Prusoff, *Biochem. Pharmacol.*, 1973, **22**, 3099–3108.
28. Epik, Version 2.6, Schrödinger, LLC, New York, NY, 2013.
29 M. Nowak, M. Kołaczkowski, M. Pawłowski and A. J. Bojarski, *J. Med. Chem.*, 2006, **49**, 205–214.
30 Z. Deng, C. Chuaqui and J. Singh, *J. Med. Chem.*, 2004, **47**, 337–344.
31 J. Witek, K. Rataj, S. Mordalski, S. Smusz, T. Kosciolek and A. J. Bojarski, *J. Cheminform.*, 2013, **5**, P28.
32. Nonius (1998). COLLECT. Nonius BV, Delft, The Netherlands.

33 Z. Otwinowski and W. Minor, *Macromol. Crystallogr. part A*, 1997, **276**, 307–326.

34. Agilent 2011 CrysAlisPro. Agilent Technologies UK Ltd. Yarnton, England.

5 35 G. M. Sheldrick, *Acta Crystallogr. A.*, 2008, **64**, 112–122.

36 L. J. Farrugia, *J. Appl. Crystallogr.*, 1999, **32**, 837–838.

37 C. F. Macrae, I. J. Bruno, J. A. Chisholm, P. R. Edgington, P. McCabe, E. Pidcock, L. Rodriguez-Monge, R. Taylor, J. van de Streek and P. A. Wood, *J. Appl. Crystallogr.*, 2008, **41**, 466–470.

10

RSC Advances Accepted Manuscript